Vol 454 | 14 August 2008 | doi:10.1038/nature07131

LETTERS

Inner-core shear-wave anisotropy and texture from an observation of PKJKP waves

James Wookey[1] & George Helffrich[1]

Since the discovery of the Earth's core a century ago[1], and the subsequent discovery[2] of a solid inner core (postulated to have formed by the freezing of iron[3]) seismologists have striven to understand this most remote part of the deep Earth. The most direct evidence for a solid inner core would be the observation of shear-mode body waves that traverse it, but these phases are extremely difficult to observe. Two reported observations in short-period data[4,5] have proved controversial[6]. Arguably more successful have been studies of longer-period data[6,7], but such averaging limits the usefulness of the observations to reported sightings. We present two observations of an inner-core shear-wave phase at higher frequencies in stacked data from the Japanese High-Sensitivity Array, Hi-Net[8]. From an analysis of timing, amplitude and waveform of the 'PKJKP' phase we derive constraints on inner-core compressional-wave velocity and shear attenuation at about 0.3 Hz which differ from standard isotropic core models[9]. We can explain waveform features and can partially reconcile the otherwise large differences between core wavespeed and attenuation models that our observations apparently suggest if we invoke shear-wave anisotropy in the inner core. A simple model of an inner core composed of hexagonal close-packed iron with its *c* axis aligned perpendicular to the rotation axis[10] yields anisotropy that is compatible with both the shear-wave anisotropy that we observe and the well-established 3 per cent compressional-wave anisotropy.

Our primary observation comes from a single event which occurred on 22 February 2006 in Mozambique, at an epicentral distance of 113.7° degrees from the centre of Hi-Net[8] (Fig. 1). This was a shallow event with a moment magnitude $M_w = 7.0$. For such a large, shallow event the source time function is remarkably impulsive (see Supplementary Fig. 1). Phase-weighted stacks[11] (Fig. 2) show very clear PKKPab, pPKKPab, PKiKP and pPKiKP arrivals, and weak PKKPbc and pPKKPbc. The separation between the primary arrivals and the depth phases best fit an event 14 km deep. Figure 2e shows the time–slowness window for PKJKP as predicted by the Earth model ak135 (ref. 9) and a clear arrival is observed. We are also able to match the arrival with synthetics (Fig. 3). As this phase arrives very close to the ak135 prediction, we suggest that this Earth model provides an accurate average inner-core shear-wave velocity. We also have made a second observation of PKJKP, from a 2007 event on the mid-Atlantic ridge, but a complex wavetrain precludes further useful analysis (see Supplementary Figs 7–8).

The PKJKP waveform presented in Fig. 3 shows another interesting feature: an arrival about 7 s after PKJKP (and 3 s after pPKJKP). This cannot be sPKJKP or another near-source converted phase, as no such phase is observed for PKKPab or PKiKP, which have very similar upper-mantle ray paths (Fig. 2). Furthermore, sPKJKP would leave a shallow event almost vertically, so the conversion to a P-wave at the free surface would be extremely weak. We interpret this secondary phase as the effect of inner-core seismic anisotropy (see Supplementary Information). Seismic anisotropy is the variation of seismic wavespeed with direction, which has been observed for the inner core using P-wave and normal mode data (see, for example, ref. 12 and references therein). When a shear-wave encounters an anisotropic medium it is split into two components whose polarizations are defined by the symmetry of the medium, and which will separate in time as they propagate through the region. In our scheme, this would lead to two distinct PKJKP phases (which we denote PKJKP1

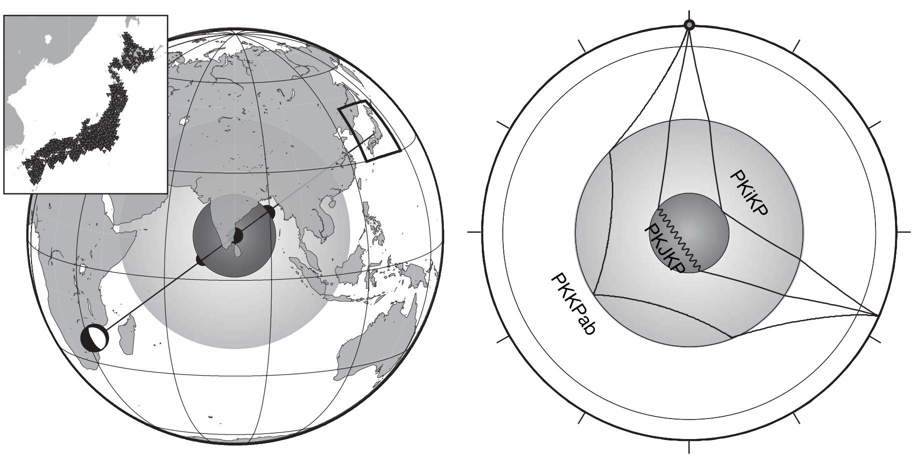

Figure 1 | Source, ray path and receiver geometry. We searched for evidence of PKJKP in records at the Japanese Hi-Net array (inset) of the $M_w = 7.0$ shallow event (depth ~14 km) on 22 February 2006 in Mozambique. The epicentral distance to the centre of the array is 113.7°. The right panel shows the ray paths for PKKPab, PKiKP and PKJKP at this distance (straight lines are P-wave segments, wavy lines are S-wave).

[1]Department of Earth Sciences, University of Bristol, Wills Memorial Building, Queens Road, BS8 1RJ, UK.

and PKJKP2). This has been predicted[12,13], but never before observed. Figure 3 shows the degree of splitting expected for shear-wave anisotropy between 0 and 2%; to explain the delay we observe requires an anisotropy of ~1% averaged across the propagation path through the inner core.

The simplest model proposed to explain the bulk anisotropy of the inner core is the alignment of iron crystals[12,13]. It has even been suggested that the inner core might be a single crystal of hexagonal close-packed (h.c.p.) iron[13]. The anisotropy that we measure is small compared with those predicted for single-crystal iron at inner-core conditions[10,14] (up to ~20%; see Supplementary Fig. 10). To explain our inferred shear-wave anisotropy as well as the much better-established P-wave anisotropy, we have explored a range of simple textural models for these elastic constants. The models are a series of orientations and rotational averages of h.c.p. and body-centred cubic (b.c.c.) iron, to provide an estimate of the aggregate elasticity (and hence anisotropy). These models are motivated by different ideas of crystal alignment due to dendritic growth during solidification[15,16] or post-solidification deformation[15,17,18]. Figure 4 outlines these mechanisms. Models tested are given in Supplementary Table 1

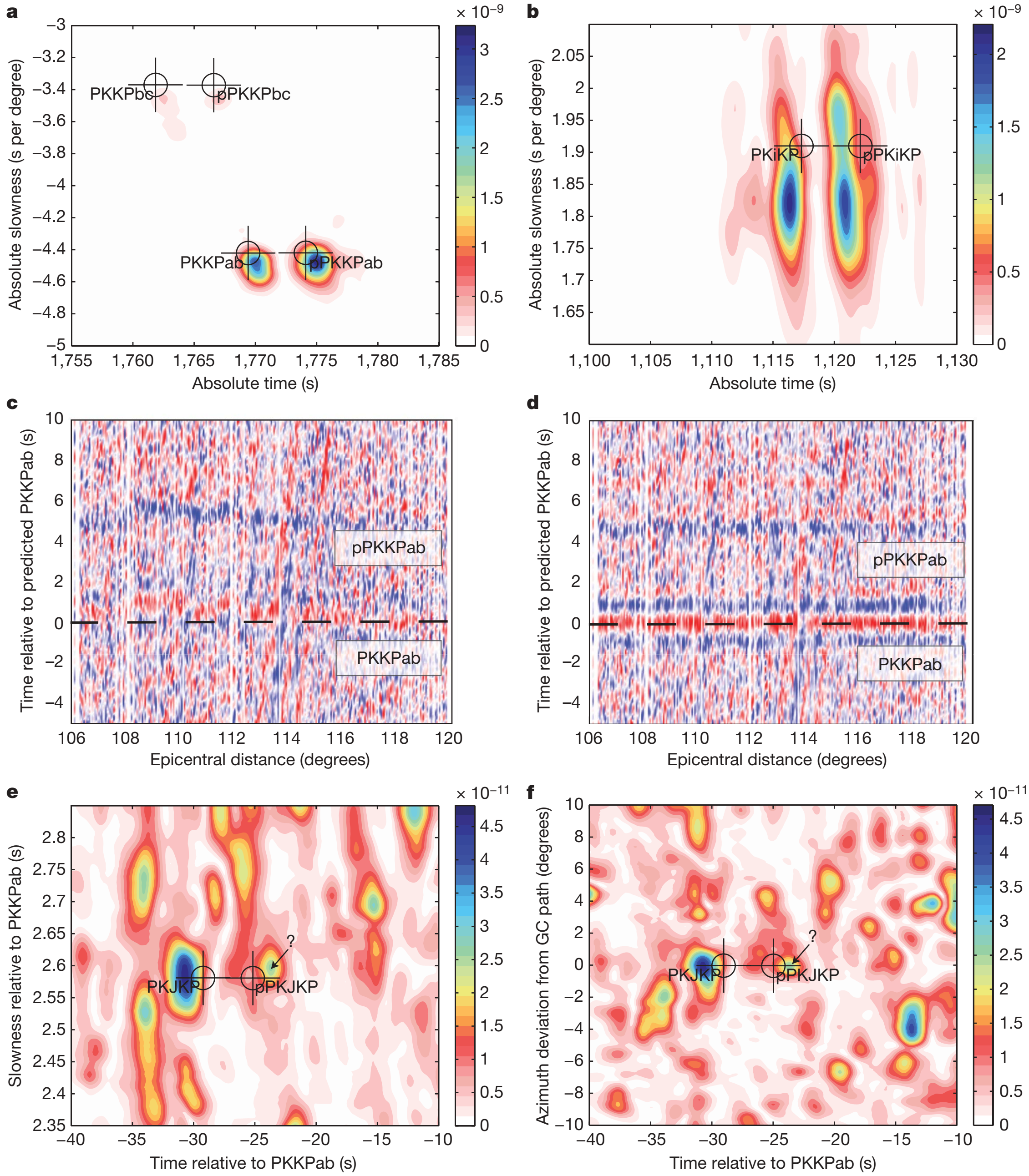

Figure 2 | Seismic data. **a**, **b**, Vespagrams for the PKKPab and PKiKP time–slowness windows, respectively. The colour scale represents the amount of energy across all the traces at a given time and slowness. These vespagrams are calculated using a phase-weighted slant stack[11]. Crosshairs denote predicted times and slowness from ak135 (ref. 9) for various core phases. Clear maxima associated with PKKPab, pPKKPab, PKiKP and pPKiKP arrivals are visible, with weaker maxima for PKKPbc and pPKKPbc. **c**, Time window for PKKPab in the unstacked data. Because PKKPab is clearly visible we use it as reference phase to calculate a receiver-side static time correction[30], and **d** shows this correction applied to PKKPab. **e**, Time–slowness window (relative to the PKKPab reference phase) where PKJKP is predicted to arrive. A clear maximum can be seen ~1.5 s before the prediction, at the correct slowness to within the resolution of the array (~0.05 s per degree). There is also energy near the time predicted for pPKJKP, although this is low amplitude (near the noise level) and poorly constrained in slowness. **f**, Azimuthal slant stack, at a fixed slowness of 2.6 s per degree. This shows that the maximum identified as PKJKP arrives within 0.2° of the (major arc) great circle path. A second peak is also seen at the slowness of PKJKP (denoted by the question mark).

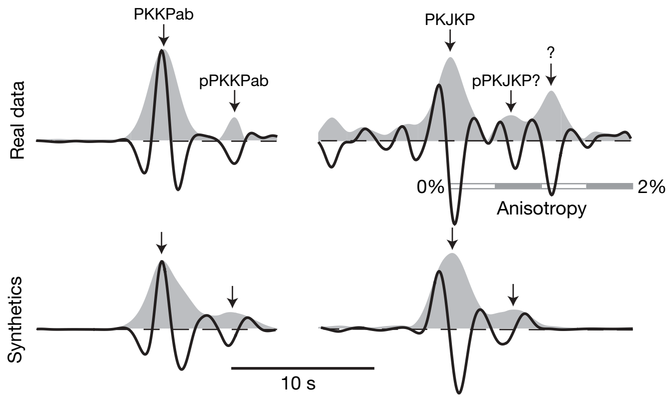

Figure 3 | Real (top) and synthetic waveforms (bottom). These are phase-weighted slant stacks at the peak slownesses for PKKPab and PKJKP. The shaded area is the envelope function of the trace. Given the uncertainty in relative amplitudes from moment tensor solutions[32], in order to match the observed amplitude ratio of between PKKPab and pPKKPab in the real data, a taper of value 0.25 is applied to the PKKPab synthetics after the primary arrival. The same taper is also applied to the PKJKP synthetics. The PKJKP phase observed is the Hilbert transform of the reference PKKPab phase, as predicted. An arrival is also apparent near the correct time for pPKJKP, although this is very close to the noise level of the trace and not well constrained. The arrival denoted by the question mark may be due to shear-wave splitting by inner-core anisotropy. The scale bar shows the time lag predicted for a model of uniform anisotropy, implying that ~1% is required to explain this phase.

and Supplementary Fig. 11. A first-order picture of inner-core anisotropy shows that P-wave phases on polar raypaths traverse the region ~3% faster than those on equatorial paths[12]. The only models tested that even roughly match this constraint involve the rotational average of h.c.p. Fe with the *c* axis perpendicular to the Earth's rotation axis[10]. These models also show a shear-wave anisotropy that is roughly compatible with that inferred from our observation of PKJKP. Thus, the measured anisotropy is currently non-unique with regard to its cause (that is, depositional or deformational) but does suggest iron with h.c.p. structure to be a better prospect than iron with b.c.c. structure. Previous observations of inner-core shear-wave anisotropy come from inversions of normal-mode observations[19,20], which predict larger absolute anisotropies. The 7-s splitting we observe for PKJKP is, in fact, compatible with these (see Supplementary Information), as such models predict a change in sign of anisotropy at a radius between 400 and 800 km (see ref. 20), leading to a relatively small aggregate anisotropy along the ray path. Mechanisms to explain such variation in anisotropy, however, are more complex than the simple textural models proposed above.

Also of interest is the strength of the PKJKP arrival, which we measure using the ratio of the recorded amplitudes PKJKP and PKiKP (hereafter $R_{J/i}$) in linear slant stacks. In our data, $R_{J/i} = 0.14 \pm 0.05$, significantly larger than $R_{J/i} = 0.02$ predicted using reflectivity modelling for a model compatible with ak135. This could be due to either an increased PKJKP amplitude or a reduced PKiKP amplitude. Inner-core anisotropy might affect PKJKP and PKiKP amplitudes by altering the reflection and coefficients at the inner-core boundary (ICB). For example we find, using elastic constants from ref. 14, that the ratio of PKJKP to PKiKP amplitude can vary significantly: up to a factor of 25 depending on the degree of alignment and orientation at the ICB (see Supplementary Fig. 14). This has also been suggested to explain observations of anomalous amplitudes of PKPdf phases[21]. As this effect alone explains both waveform features and the observed $R_{J/i}$ without requiring modification of the core's isotropic properties, we favour it. But to test whether we can in fact reconcile our observation with an isotropic, spherically symmetric model of the inner core, we have also run a suite of synthetics varying the seismic velocity (V_P and V_S), density and Q_S (the shear-wave 'quality' factor, also sometimes called Q_μ) in the inner core (see Supplementary Information). We find that $R_{J/i}$ depends most strongly on V_P of the inner core at the ICB (predominantly through the amplitude of PKiKP), with a weaker but significant dependence on Q_S (through the amplitude of PKJKP). The influence of V_S and density (at least within bounds compatible with normal-mode data) is negligibly weak. Supplementary Fig. 13 shows the variation in $R_{J/i}$ with inner-core V_P and Q_S, identifying the distribution of models consistent with our measured $R_{J/i}$. This shows that to reconcile our measured $R_{J/i}$ with an isotropic one-dimensional model of the inner core requires a much higher Q_S than is inferred from normal-mode studies, a considerably reduced V_P (at least near the ICB), or a more moderate combination of the two. For example, in order that Q_S be compatible with the normal-mode

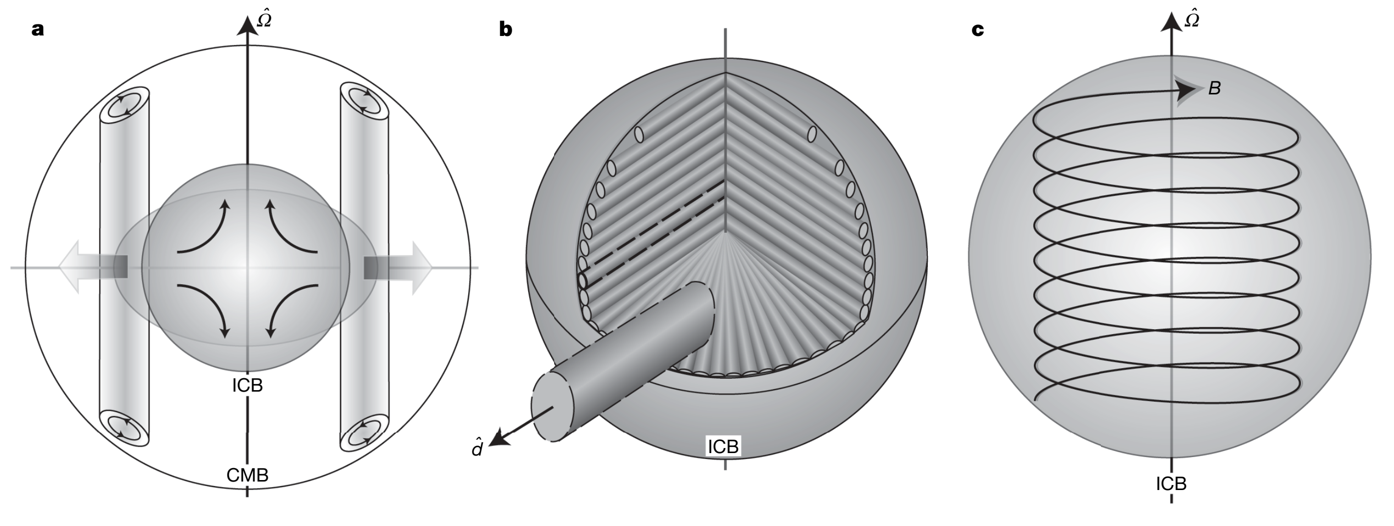

Figure 4 | Possible causes of crystal alignment in the inner core. **a**, Compressional and tensional deformation due to non-uniform growth. Outer-core convection in Taylor columns[33] leads to larger equatorial heat-flux, promoting freezing at the ICB in these regions. This oblateness is dynamically unstable, leading to deformation[17] symmetrically about the rotation axis (Ω). CMB, core–mantle boundary. **b**, Crystal alignment due to dendritic solidification. As liquid iron freezes onto the ICB, dendrite structures might be formed[16] and could persist deep into the inner core. In this case crystals would be oriented relative to the dendrite long axes (d), which we assume to be perpendicular to Ω. Solid-state, inward axial flow modifies orientation (Supplementary Table 1 and Fig. 11). **c**, Alignment due to Maxwell stresses (after ref. 18). In this model, stresses exerted by the Earth's magnetic field (B) re-orient crystals of inner-core iron, leading to large-scale texturing.

measurements of ref. 22, the P-wave velocity increase at the ICB must be of the order of 0.3 km s^{-1} (compared with 0.75 km s^{-1} in ak135). A global degree-1 asymmetry of P-wave speed (with a deviation from the reference model of −0.7 to +0.2%) in the outermost part of the inner core has been documented[23,24], but this variation is much smaller than our observations require. A strong variation in PKiKP amplitude has also been observed by using P or PcP as a reference phase[25–27]. It is also possible, however, that attenuation values derived from normal modes are not appropriate at body-wave frequencies (see refs 28, 29 and Supplementary Information). The amplitude spectrum of the PKJKP (see Supplementary Fig. 9) also suggests that Q_S in the inner core might be higher than previously estimated. This is hard to reconcile with measurements of P-wave Q from PKIKP[28,29], without significant bulk attenuation, and perhaps a layered Q structure in the inner core. The influence of scattering attenuation may also be important[29]. These issues are discussed further in the Supplementary Information, but drawing firm conclusions as to the causes will require more observations than provided by a single measurement. There are several factors that might influence the amplitudes of PKJKP and PKiKP beyond those that may be tested by our modelling methodology, including the focusing/defocusing effects of ICB topography or inner-core velocity heterogeneity. However, we believe that the simplest explanation remains the effect of anisotropy.

To test these ideas further requires more PKJKP observations at different traversal directions across the inner core. We believe that as the new generation of large-aperture dense array experiments such as Hi-Net and the nascent USArray begin to accumulate data, PKJKP should become a more routinely detected phase. Such accumulated observations will probe other areas of the inner core to assess the possible hemispheric variation in its shear anisotropy; our observations are confined to the quasi-western hemisphere[24]. This will provide stronger constraints on the depth extent of texturing and inner-core growth through time.

METHODS SUMMARY

Our data comprise 704 short-period Hi-Net[8] records from borehole seismometers sited around the Japanese Islands. We use PKKPab as a reference phase to calculate a receiver-side static time correction[30]. Data are initially bandpass filtered between 0.05 and 2 Hz, to remove high-frequency noise. A power-2 phase-weighted slant stack[11] is applied and the data are bandpass filtered again between 0.05 and 0.5 Hz to smooth the spectra, and a trace envelope function is derived. Figure 2e shows the time–slowness window for PKJKP as predicted by ak135 (ref. 9). A clear energy pulse can be observed at a slowness which is indistinguishable from the model-predicted slowness, and ~1.5 s earlier than the predicted arrival time. Azimuthal stacking shows a deviation of $<0.2^\circ$ from the major arc great circle path (Fig. 2f). We interpret this phase to be PKJKP. We are also able to match the arrival with reflectivity method[31] synthetics for a one-dimensional isotropic Earth model[9] (Fig. 3). The PKJKP phase observed is the Hilbert transform of the reference PKKPab phase, as predicted. Further tests are detailed in the Supplementary Information. For amplitude measurements, linear slant stacks are used to avoid biasing by phase weighting. Amplitude error bounds are estimated from the signal-to-noise ratio of the PKJKP peak; those of PKiKP are negligible in comparison. A correction is also made for the moment tensor.

Full Methods and any associated references are available in the online version of the paper at www.nature.com/nature.

Received 22 November 2007; accepted 28 May 2008.

1. Oldham, R. D. The constitution of the interior of the Earth, as revealed by earthquakes. *Q. J. Geol. Soc. Lond.* **62,** 456–475 (1906).
2. Lehmann, I. P′. *Bur. Centr. Sismol. Int. A* **14,** 87–115 (1936).
3. Birch, F. The alpha–gamma transformation of iron at high pressures, and the problem of the Earth's magnetism. *Am. J. Sci.* **238,** 192–211 (1940).
4. Julian, B. R., Sheppard, R. M. & Davies, D. PKJKP. *Nature* **235,** 317–318 (1972).
5. Okal, E. A. & Cansi, Y. Detection of PKJKP at intermediate periods by progressive multi-channel correlation. *Earth Planet. Sci. Lett.* **164,** 23–30 (1998).
6. Deuss, A., Woodhouse, J. H., Paulssen, H. & Trampert, J. The observation of inner core shear waves. *Geophys. J. Int.* **142,** 67–73 (2000).
7. Cao, A. M., Romanowicz, B. & Takeuchi, N. An observation of PKJKP: Inferences on inner core shear properties. *Science* **308,** 1453–1455 (2005).
8. Obara, K., Kasahara, K., Hori, S. & Okada, Y. A densely distributed high-sensitivity seismograph network in Japan: Hi-net by National Research Institute for Earth Science and Disaster Prevention. *Rev. Sci. Instrum.* **76,** 21301–1–12 (2005).
9. Kennett, B. L. N., Engdahl, E. R. & Buland, R. Constraints on seismic velocities in the Earth from traveltimes. *Geophys. J. Int.* **122,** 108–124 (1995).
10. Steinle-Neumann, G., Stixrude, L., Cohen, R. E. & Gülseren, O. Elasticity of iron at the temperature of the Earth's inner core. *Nature* **413,** 57–60 (2001).
11. Schimmel, M. & Paulssen, H. Noise reduction and detection of weak, coherent signals through phase-weighted stacks. *Geophys. J. Int.* **130,** 497–505 (1997).
12. Song, X. Anisotropy of the Earth's inner core. *Rev. Geophys.* **35,** 297–314 (1997).
13. Stixrude, L. & Cohen, R. E. High-pressure elasticity of iron and anisotropy of Earth's inner core. *Science* **267,** 1972–1975 (1995).
14. Vočadlo, L. Ab initio calculations of the elasticity of iron and iron alloys at inner core conditions: evidence for a partially molten inner core? *Earth Planet. Sci. Lett.* **254,** 227–232 (2007).
15. Barrett, C. & Massalski, T. *Structure of Metals: Crystallographic Methods Principles and Data* 3rd rev. edn (Pergamon, Oxford, 1980).
16. Bergman, M. I., MacLeod-Silberstein, M., Haskel, M., Chandler, B. & Akpan, N. A laboratory model for solidification of Earth's core. *Phys. Earth Planet. Int.* **153,** 150–164 (2005).
17. Yoshida, S., Sumita, I. & Kumazawa, M. Growth model of the inner core coupled with the outer core dynamics and the resulting elastic anisotropy. *J. Geophys. Res.* **101,** 28085–28103 (1996).
18. Buffett, B. A. & Wenk, H. R. Texturing of the Earth's inner core by Maxwell stresses. *Nature* **413,** 60–63 (2001).
19. Tromp, J. Support for anisotropy of the Earth's inner core from free oscillations. *Nature* **366,** 678–681 (1993).
20. Beghein, C. & Trampert, J. Robust normal mode constraints on inner-core anisotropy from model space search. *Science* **299,** 552–555 (2003).
21. Creager, K. Anisotropy of the inner core from differential travel-times of the phases PKP and PKIKP. *Nature* **356,** 309–314 (1992).
22. Widmer, R., Masters, G. & Gilbert, F. Spherically symmetric attenuation within the Earth from normal mode data. *Geophys. J. Int.* **104,** 541–553 (1991).
23. Kaneshima, S. Mapping heterogeneity of the uppermost inner core using two pairs of core phases. *Geophys. Res. Lett.* **23,** 3075–3078 (1996).
24. Tanaka, S. & Hamaguchi, H. Degree one heterogeneity and hemispherical variation of anisotropy in the inner core from PKP(BC)-PKP(DF) times. *J. Geophys. Res.* **102,** 2925–2938 (1997).
25. Koper, K. D. & Pyle, M. L. Observations of PKiKP/PcP amplitude ratios and implications for Earth structure at the boundaries of the liquid core. *J. Geophys. Res.* **109,** B03301 (2004).
26. Krasnoshchekov, D. N., Kaazik, P. B. & Ovtchinnikov, V. M. Seismological evidence for mosaic structure of the surface of the Earth's inner core. *Nature* **435,** 483–487 (2005).
27. Koper, K. D. & Dombrovskaya, M. Seismic properties of the inner core boundary from PKiKP/P amplitude ratios. *Earth Planet. Sci. Lett.* **237,** 680–694 (2005).
28. Romanowicz, B. & Durek, J. J. in *Earth's Deep Interior: Mineral Physics and Tomography from the Atomic to the Global Scale* (eds Karato, S., Forte, A., Liebermann, R., Masters, G. & Stixrude, L.) *Geophys. Monogr.* 117, 161–179 (Am. Geophys. Un., Washington DC, 2000).
29. Cormier, V. F. & Li, X. Frequency-dependent seismic attenuation in the inner core 2. A scattering and fabric interpretation. *J. Geophys. Res.* **107,** 2362 (2002).
30. Rawlinson, N. & Kennett, B. L. N. Rapid estimation of relative and absolute delay times across a network by adaptive stacking. *Geophys. J. Int.* **157,** 332–340 (2004).
31. Mueller, G. The reflectivity method; a tutorial. *J. Geophys.* **58,** 153–174 (1985).
32. Helffrich, G. R. How good are routinely determined focal mechanisms? Empirical statistics based on a comparison of Harvard, USGS and ERI moment tensors. *Geophys. J. Int.* **131,** 741–750 (1997).
33. Zhang, K. Nonlinear magnetohydrodynamic convective flows in the Earth's fluid core. *Phys. Earth Planet. Inter.* **111,** 93–103 (1999).

Supplementary Information is linked to the online version of the paper at www.nature.com/nature.

Acknowledgements We thank L. Vočadlo, M. Kendall, M. Bergman and A. Deuss for discussions, C. Beghein for providing her inner-core anisotropy models and L. Stixrude for a review. J.W. was supported by a NERC postdoctoral fellowship grant.

Author Contributions Data analysis and modelling was undertaken by J.W., initiated by, and in consultation with, G.H. Phase-weighted stacking code and inner-core texture models were developed by G.H. Manuscript and figures were produced by J.W.

Author Information Reprints and permissions information is available at www.nature.com/reprints. Correspondence and requests for materials should be addressed to J.W. (j.wookey@bristol.ac.uk).

METHODS

Our data comprise 704 short-period Hi-Net[8] records from borehole seismometers sited around the Japanese Islands. As the PKKPab arrival is very clear, we use it as a reference phase to calculate a receiver-side static time correction[30]. Data are initially bandpass filtered between 0.05 and 2 Hz, to remove high-frequency noise. A power-2 phase-weighted slant stack[11] is applied and the data are bandpass filtered again between 0.05 and 0.5 Hz to smooth the spectra. We assume a linear moveout between PKJKP and PKKPab in slant stacking. The maximum deviation from this is of the order of 0.1 s, much less than the dominant period of the phase, and may be neglected. Finally the trace envelope function is derived. Figure 2e shows the time–slowness window for PKJKP as predicted by ak135 (ref. 9). A clear energy pulse can be observed at a slowness which is indistinguishable from the model-predicted slowness (we calculate the slowness resolution of the array to be about 0.05 s per degree; see Supplementary Fig. 2), and ~1.5 s earlier than the predicted arrival time. We interpret this phase to be PKJKP. Other phases that have previously been identified as problematic (for example, PcPPKIKP, PcPPKiKP and PKKPdf; see refs 4, 5, 7) are predicted to arrive well separated in time or slowness or both. Further evidence for the arrival being PKJKP comes from slant stacking with varying azimuth, with a fixed slowness of 2.6 s per degree relative to PKKPab (Fig. 2f). This shows that the arrival has maximum amplitude at a deviation of less than 0.2° from the great circle path and that it arrives on the major arc. We are also able to match the arrival with synthetics. We use reflectivity method[31] synthetics for a one-dimensional isotropic Earth model[9]. These are processed identically to real data, except a static correction is unnecessary. Figure 3 shows the comparison of the slant-stacked waveform with synthetics. The PKJKP phase observed is the Hilbert transform of the reference PKKPab phase, as is predicted by the synthetics. A weak phase is also observed at the correct time for a source 14 km deep as predicted by PKKPab and PKiKP. Further tests are detailed in the Supplementary Information. To compare the shear-wave splitting we infer with previous, normal-mode derived models we calculate[34] accrued lag-time between SH and SV phases, assuming no perturbation of the isotropic ray path. This is done for the minimum, maximum and mean models of ref. 20. We find that the 7-s splitting we measure is compatible with the range of normal-mode models (see Supplementary Information). For amplitude measurements, linear slant stacks are used to avoid biasing by phase weighting. Amplitude error bounds are estimated from the signal-to-noise ratio of the PKJKP peak; those of PKiKP are an order of magnitude smaller because of a much larger amplitude. A correction is also made for the moment tensor.

34. Thomsen, L. Weak elastic anisotropy. *Geophysics* **51**, 1954–1966 (1986).